

Single-nucleon transfer to unbound states in the ${}^4\text{He}(\alpha,t){}^5\text{Li}$ reaction at incident energies of 120, 160, and 200 MeV

G. F. Steyn,¹ S. V. Förtsch,¹ A. A. Cowley,² S. Karataglidis,³ R. Lindsay,⁴ J. J. Lawrie,¹ F. D. Smit,¹ and R. T. Newman¹

¹National Accelerator Center, Faure, 7131, South Africa

²Department of Physics, University of Stellenbosch, Stellenbosch, 7600, South Africa

³Theory Group, TRIUMF, 4004 Wesbrook Mall, Vancouver, British Columbia, Canada V6T 2A3

⁴Department of Physics, University of the Western Cape, Bellville, 7535, South Africa

(Received 12 December 1997)

The ${}^4\text{He}(\alpha,t){}^5\text{Li}(\text{g.s.})$ reaction was investigated at incident energies of 120, 160, and 200 MeV in order to resolve discrepancies found between previous measurements and theoretical predictions for the analogous reaction ${}^4\text{He}(\alpha,{}^3\text{He}){}^5\text{He}(\text{g.s.})$ at these energies. The line shapes of the ${}^5\text{Li}$ ground-state resonance in the measured triton energy spectra are well reproduced by distorted-wave Born approximation (DWBA) calculations. Cluster-core optical potentials, which yield better overall agreement both for α - α elastic scattering and for the single-nucleon transfer reactions, are presented. It is shown that the previously observed discrepancies in magnitude between measured and calculated cross sections by a factor of ~ 2 can be improved by employing spectroscopic factors obtained from a realistic shell model for the transitions to the final mass-3 and mass-5 systems. [S0556-2813(98)06304-3]

PACS number(s): 25.55.Hp, 24.10.Ht, 27.10.+h, 24.10.Eq

I. INTRODUCTION

Cross sections for reactions leading to ${}^5\text{He}(\text{g.s.})$ and ${}^5\text{Li}(\text{g.s.})$ residual systems can be obtained from singles measurements when the relationship between the energy and scattering angle of an observed stable ejectile is constrained by two-body kinematics. This has been exploited in an investigation of the ${}^4\text{He}(\alpha,{}^3\text{He}){}^5\text{He}(\text{g.s.})$ reaction at 118 MeV [1] as well as at higher incident energies of 158 and 200 MeV [2]. The measured ${}^3\text{He}$ energy spectra of these authors exhibit a strong resonance peak corresponding to the unbound ${}^5\text{He}$ ground state, which is a resonant neutron state with a width of $\Gamma=0.60$ MeV and a resonance energy of $\epsilon=0.89$ MeV [3]. It was shown that the DWBA could be employed with reasonable success in predicting the shape of the angular distribution of this reaction. The absolute magnitude of the cross sections, however, is overpredicted by a factor of ~ 2 .

In this paper we report on an experimental investigation of the ${}^4\text{He}(\alpha,t){}^5\text{Li}(\text{g.s.})$ reaction at incident energies of 120, 160, and 200 MeV. The structure of ${}^5\text{Li}$, the ground state of which is a resonant proton state with a width of $\Gamma=1.5$ MeV and a resonance energy of $\epsilon=1.97$ MeV [3], is comparable to that of ${}^5\text{He}$. Thus the two possible reactions involving the transfer of only a single nucleon when two ${}^4\text{He}$ nuclei interact are also expected to exhibit similar behavior. However, different depths of the real central potential are required for the α -nucleon interaction to correctly locate the respective ${}^5\text{He}$ and ${}^5\text{Li}$ ground-state resonances in the calculated DWBA energy spectra. This difference may provide information on the sensitivity to the parameters of the α -nucleon interaction, which could in principle be responsible for the discrepancy in magnitude between measured and calculated cross sections. On the other hand, the choice of optical potentials for generating the distorted waves may also be suspect. Conventional Woods-Saxon potentials, for example,

are known to be inadequate in the description of α -elastic scattering in certain energy and mass regimes [4]. This may also be the case for the entrance channel in the transfer reactions of the present study. For the exit channels the situation is even more uncertain due to the total but inevitable lack of experimental elastic scattering data involving mass-5 nuclei.

Parameter values for the recently published even-even cluster-core potentials of Buck, Merchant, and Perez [4] were extracted by means of optical model fits to α - α elastic scattering data. These potentials were employed in the DWBA calculations in an effort to at least obtain an alternative to the Woods-Saxon potentials used previously. Although the results obtained with an additional set of phenomenological potentials can by no means give decisive answers as to the degree of sensitivity to the choice of optical potentials, they may nevertheless give one some indication thereof. The parameters of the cluster-core potentials are presented as functions of energy for the region 120 to 200 MeV.

The cross sections for single-nucleon transfer to the mass-5 ground states are dominated by the contribution from the $1p_{3/2}$ state, with the contribution from the $1p_{1/2}$ state only of the order of 1%. Shell model calculations were performed for these reactions, yielding a somewhat lower spectroscopic factor for the transfer to the $1p_{3/2}$ state of the mass-5 system than previously assumed. Similarly, a shell model prediction for the spectroscopic factor of the transition involving the $1s_{1/2}$ state of the mass-3 ejectiles produced in these reactions are found to be lower than the value used in previous work. It was found [1,2] that the discrepancy between experimental and theoretical cross sections is reduced when these more refined spectroscopic factors are introduced in the theoretical calculations of the present study. The overall agreement is encouraging, indicating that good DWBA predictions are feasible for single-nucleon transfer reactions to unbound states even for very light nuclear systems, such

as when two α particles interact.

The experimental details for the ${}^4\text{He}(\alpha, t){}^5\text{Li}(\text{g.s.})$ measurements are presented in Sec. II, aspects of the data analysis in Sec. III, extraction of optical potential parameters in Sec. IV, details of the DWBA calculations in Sec. V, and the results are discussed in Sec. VI. Finally, a summary and conclusions are presented in Sec. VII.

II. EXPERIMENTAL PROCEDURE

The experimental setup used for the ${}^4\text{He}(\alpha, t){}^5\text{Li}(\text{g.s.})$ measurements is similar to the system used previously in our investigation of the ${}^4\text{He}(\alpha, {}^3\text{He}){}^5\text{He}(\text{g.s.})$ reaction [2] at the National Accelerator Center. Therefore only a short description will be given here. The helium target gas (>99.995% purity) was contained in a 100 mm-diameter gas cell, filled to a nominal absolute pressure of 1.5 bar at room temperature. The pressure and temperature of the target gas were monitored continuously to a precision of better than 1%. The target was bombarded inside a scattering chamber of 1.5 m in diameter with α -particle beams of 120.4, 159.3, and 202.6 MeV, respectively. The uncertainty in the quoted beam energies is not more than 0.5 MeV. An active double-aperture collimator system was used to define the effective target length and a solid angle of 0.8 msr, with an angular resolution of 1.7° . The detector telescope consisted of a 2 mm thick Si surface-barrier ΔE detector, followed by a NaI stopping detector. Standard ΔE - E techniques were used for particle identification. Gain drift in the NaI detector was monitored by means of a LED pulser and corrected for. Data were collected at 1° intervals, covering the laboratory angular region 10° – 50° . Based on the various experimental uncertainties, the cross sections are estimated to be accurate to within a systematic error of 5%.

III. DATA ANALYSIS

Center of mass differential cross sections for the transfer reaction were extracted from the measured triton energy spectra. Similar to the procedure followed in Refs. [1,2], an energy-integrated differential cross section can be defined by

$$\sigma_{\epsilon^*}(\theta) = \int_0^{\epsilon^*} \sigma(\epsilon, \theta) d\epsilon, \quad (1)$$

where the integration is over the relative α - p energy in ${}^5\text{Li}$. The relationship between ϵ and the energy of the triton ejectile is given by two-body kinematics. An upper integration limit of $\epsilon^* = 6$ MeV was adopted due to the larger width of the ${}^5\text{Li}(\text{g.s.})$ resonance. [Previously, a value of $\epsilon^* = 5$ MeV was adopted for the ${}^4\text{He}(\alpha, {}^3\text{He}){}^5\text{He}(\text{g.s.})$ reaction [1,2]. These integration limits give similar peak-to-tail ratios for the two reactions.] Further details of the data analysis can be found in Ref. [2].

IV. CLUSTER-CORE OPTICAL POTENTIALS

The even-even cluster-core potential of Buck, Merchant, and Perez [4] has been incorporated in the following expression:

$$V_{opt} = -V_0 f(r, x, r_0, a_0) - iWh(r, r_w, a_w) + V_c, \quad (2)$$

where

$$f(r, x, r_0, a_0) = \frac{x}{\{1 + \exp[(r - r_0 A^{1/3})/a_0]\}} + \frac{1 - x}{\{1 + \exp[(r - r_0 A^{1/3})/3a_0]\}^3}, \quad (3)$$

and

$$h(r, r_w, a_w) = \{1 + \exp[(r - r_w A^{1/3})/a_w]\}^{-1}. \quad (4)$$

V_c is the Coulomb potential, taken to be that acting between a point projectile and a spherical target with uniform charge and radius $r_c A^{1/3}$, where A is the mass of the target nucleus. These expressions have been incorporated into the optical model code SNOOPY8 [5] in order to search for parameter values by fitting of calculated cross sections to α - α elastic scattering data. For this purpose the data measured at 120 MeV [6], 140 MeV [7], 160 MeV, and 200 MeV [2] (see Fig. 1) were used.

Initial parameter values for the real part of the nuclear potential were taken from Ref. [4], which reproduced the quasibound 0^+ state of ${}^8\text{Be}$ at $Q = 92$ keV as well as α - α elastic scattering phase shifts up to 40 MeV incident energy in the center of mass system. These values are $x = 0.33$, $a_0 = 0.73$ fm, $r_0 = 1.06$ fm, and $U_0 = 54$ MeV, where the relationship between V_0 and U_0 can be found from a mass-symmetric formulation of the cluster-core potential [4] and Eq. (2) to be given by

$$V_0 = \left(\frac{A_p A}{A_p + A - 1} \right) \frac{U_0}{f(0, x, r_0, a_0)}, \quad (5)$$

where A_p is the cluster mass, associated with the projectile in our application. The parameters of the imaginary Woods-Saxon wells of Ref. [2] were taken as starting values for the search of the absorptive part of the potential. Initially, all seven parameters were allowed to vary in unconstrained ‘‘best fit’’ searches. The parameter x appeared to remain stable from the outset, with values ranging only between 0.32 and 0.34 once convergence criteria were satisfied. It was consequently held fixed at an average value of 0.33. Within the limitations imposed by continuous ambiguities [8], a better agreement could nevertheless be found with r_0 values slightly lower than 1 fm for the 200 MeV data, especially in the region near 60° (c.m.) where a local minimum appearing in the calculated angular distribution becomes less pronounced (see Fig. 1). Consequently r_0 was fixed at a value of 0.97 fm. Weak energy dependences were found for the remaining geometric parameters and linear least-squares fits were performed to determine these dependences phenomenologically. We also found that for the real and imaginary potential strengths, similar energy dependences to those of Schwandt *et al.* [9] for proton-nucleus potentials could be employed with minimal deterioration to the best fits obtained with the 140, 160, and 200 MeV data. In the case of the 120 MeV data a deviation near the local minimum at about 80° (c.m.) is pronounced, but the overall agreement can still be considered to be reasonable.

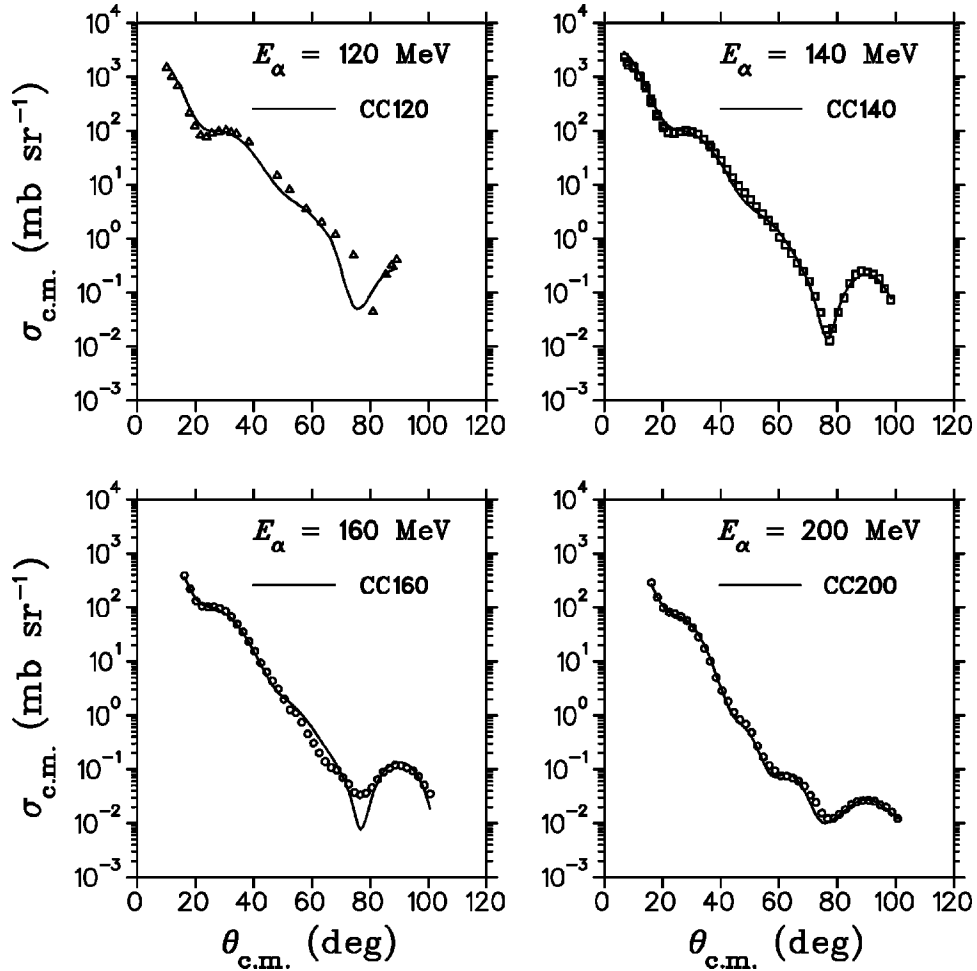


FIG. 1. Elastic scattering cross sections for $\alpha + {}^4\text{He}$ at nominal incident energies of 120, 140, 160, and 200 MeV. The open triangles are measured data taken from Ref. [6], the open squares from Ref. [7], and the open circles from Ref. [2]. The curves are optical model fits, utilizing the cluster-core potentials presented in Sec. IV and Table I.

Results of the optical model fits are shown in Fig. 1. The underprediction at the minimum near 75° in the 160 MeV case could not be eliminated in any of the parameter searches performed. The overall agreement, however, is still significantly better than that obtained previously [2] with conventional Woods-Saxon potentials. The final parameter values and/or functional expressions (with the potential strengths in MeV and the geometric parameters in fm) are given below, where T_α (in MeV) is the laboratory kinetic energy of the projectile:

$$\begin{aligned}
 V_0 &= 71.63(1 + 4.441 \times 10^{-1} \ln T_\alpha), \\
 r_0 &= 0.97, \\
 a_0 &= 0.788 - 5.528 \times 10^{-4}(T_\alpha - 120), \\
 x &= 0.33, \\
 W &= 7.8 + 3.607 \times 10^{-2}(T_\alpha - 120) \\
 &\quad + 6.162 \times 10^{-6}(T_\alpha - 120)^3, \\
 r_w &= 2.381 - 3.263 \times 10^{-3}(T_\alpha - 120), \\
 a_w &= 0.325 - 2.885 \times 10^{-4}(T_\alpha - 120).
 \end{aligned} \tag{6}$$

The applicable energy region for these potentials is $120 \leq T_\alpha \leq 200$ MeV, in which the predominant characteristics of α - α elastic scattering are reproduced.

V. CALCULATIONS

Only a very brief description of the methods used are given here since the details have been presented elsewhere [2]. DWBA calculations for the transfer reactions were performed in zero range with a version of the computer code DWUCK4 [10] that has been symmetrized to account for an entrance channel with two identical particles.

Center-of-mass double-differential cross sections are given by [11]

$$\sigma^{jl}(\epsilon, \theta) = \left(\frac{\mu k}{\pi \hbar^2} \right) \left(\frac{2j+1}{2l+1} \right) D_0^2 \sigma_{\text{DW}}^{jl}, \tag{7}$$

where μ is the reduced mass, k is the relative wave number, and ϵ is the relative energy of the α -nucleon system; j and l are the total and orbital angular momentum quantum numbers of the transferred nucleon respectively; σ_{DW}^{jl} is the

TABLE I. Summary of optical-model parameters used in this study. The cluster-core (CC) potentials are according to Eq. (6). The Woods-Saxon (WS) potentials are defined as follows: $V_{opt} = -V_0 f(r, r_0, a_0) - iWf(r, r_w, a_w) + V_c$, where $f(r, r_i, a_i) = \{1 + \exp[(r - r_i A^{1/3})/a_i]\}^{-1}$; A is the target mass; V_c is the Coulomb potential of a uniformly charged sphere of radius^a $r_c A^{1/3}$; and E_α is the incident laboratory kinetic energy.

E_α (MeV)	Pot. set	V_0 (MeV)	r_0 (fm)	a_0 (fm)	W (MeV)	r_w (fm)	a_w (fm)	Ref.	
120	WS120	115.42	1.01	0.769	7.42	2.123	0.503	[this work]	
160	WS160	95.33	1.113	0.769	9.48	2.123	0.503	[2]	
200	WS200	84.6	1.113	0.769	9.30	2.123	0.503	[2]	
E_α (MeV)	Pot. set	V_0 (MeV)	r_0 (fm)	a_0 (fm)	W (MeV)	r_w (fm)	a_w (fm)	x (fm)	Ref.
120	CC120	223.89	0.97	0.788	7.80	2.381	0.325	0.33	[this work]
160	CC160	232.77	0.97	0.767	9.54	2.255	0.314	0.33	[this work]
200	CC200	240.25	0.97	0.743	13.92	2.118	0.302	0.33	[this work]
Bound state	Pot. set	V_1 (MeV)	r_1 (fm)	a_1 (fm)	^b λ	r_c (fm)	Ref.		
	$\alpha + n$	46.71	1.25	0.65	38.0		[1,2,11]		
	$\alpha + p$	45.20	1.25	0.65	38.0	1.415	[this work]		
	³ He + n	c	1.25	0.65	38.0		[2]		
	³ H + p	d	1.25	0.65	38.0	1.3	[this work]		

^aCoulomb radius parameter $r_c = 1.3$ fm except for the $\alpha + p$ system, as indicated.

^b λ -factor for multiplying Thomas spin-orbit term.

^{c,d}Adjusted to reproduce the binding energy.

DWUCK4 cross section and D_0^2 is the usual zero-range normalization factor to correct (at least approximately) for finite-range effects.

Contributions to the ground-state of the α -nucleon system from both the $1p_{3/2}$ and $1p_{1/2}$ states were calculated for a set of ϵ values covering the region from 0 to ϵ^* and added incoherently after integration according to Eq. (1) to obtain energy-integrated differential cross sections. Equation (7) is appropriate for the single-particle shell model spectroscopic sum rule limit. However, spectroscopic factors for energy-integrated resonant final states can be treated in the same way as for bound states [12]. Therefore

$$\sigma_{\epsilon^*}(\theta) = \sum_{j', l', j, l} S_{j'l'}^{4 \rightarrow 3} S_{jl}^{4 \rightarrow 5} \int_0^{\epsilon^*} \sigma^{jl}(\epsilon, \theta) d\epsilon, \quad (8)$$

where $S_{j'l'}^{4 \rightarrow 3}$ and $S_{jl}^{4 \rightarrow 5}$ are normalizations to the spectroscopic factors for ⁴He to mass-3 and ⁴He to mass-5 states, respectively. These normalizations are introduced to take possible deviations from the single-particle sum rule into account.

Theoretical D_0^2 values were obtained from ratios of the calculated total cross section given by corresponding finite-range and zero-range DWBA calculations, assuming the ⁵Li final state to be bound by 0.1 MeV. A symmetrized version of the computer code DWUCK5 [13] was used for the finite-range calculations. Following Refs. [1,2], a real Woods-Saxon well with spin-orbit coupling [11], which fits the energy-dependence of the p - α phase shifts, was adopted for the α -nucleon interaction. As mentioned before, the real cen-

tral well depth was adjusted to correctly locate the ⁵Li ground-state resonance. Likewise, for the finite-range calculations a real Woods-Saxon well with spin-orbit coupling was also used to describe the nucleon bound state in ⁴He. In this case, however, the central well depth was adjusted to reproduce the nucleon binding energy. Bound-state wave functions were generated internally by means of the built-in prescriptions of the DWBA codes. Distorted waves for both the entrance and exit channels were generated with conventional 6-parameter Woods-Saxon potentials as well as with the cluster-core potentials presented in Sec. IV. The parameter values are listed in Table I. The 160 and 200 MeV Woods-Saxon potentials are from Ref. [2], while the 120 MeV set was obtained in this work by means of SNOOPY8 fits to the data of Ref. [6].

The spectroscopic factors were obtained from wave functions for the triton, ⁴He and ⁵Li nuclei calculated in a complete $(0+2+4)\hbar\omega$ shell model space, using the G -matrix interaction of Zheng *et al.* [14]. The binding energies obtained are -6.763 , -25.459 , and -22.201 MeV for the t , ⁴He, and ⁵Li, respectively, which agree to within 2 MeV with the experimental values [3,15]. The spectroscopic factors so obtained are 0.925 for the $1p_{3/2}$ state (stripping) and 1.738 for the $1s_{1/2}$ state (pickup), which correspond to 92.5% and 86.9% of the extreme single-particle shell model values respectively.

VI. RESULTS AND DISCUSSION

Representative examples of triton energy spectra measured at 120, 160, and 200 MeV together with corresponding

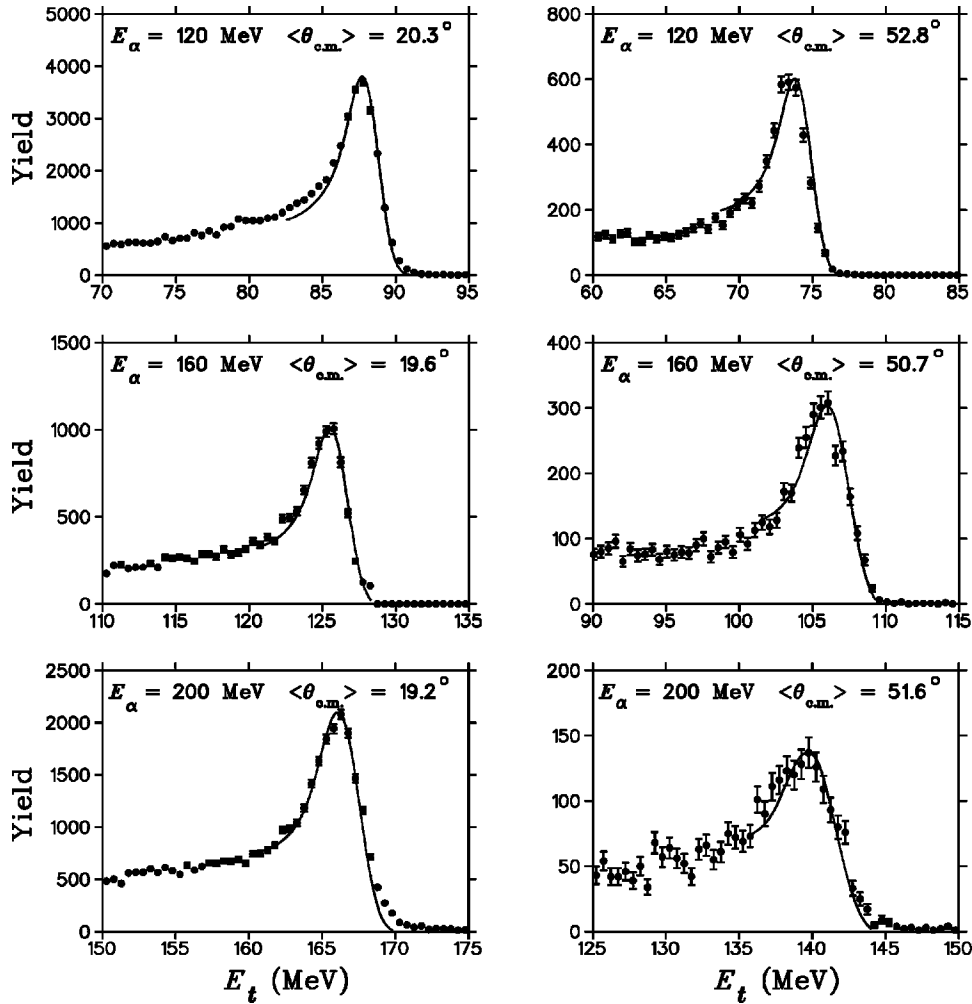


FIG. 2. Representative laboratory triton energy spectra for the ${}^4\text{He}(\alpha,t){}^5\text{Li}$ reaction at incident energies of 120, 160, and 200 MeV. The mean c.m. scattering angles indicated, $\langle \theta_{c.m.} \rangle$, correspond to lab. angles of 10.0° and 26.0° . The curves are DWBA predictions (with the cluster-core potentials of Table I) for $0 \leq \epsilon \leq 6$ MeV (see text), normalized arbitrarily to the measured data.

DWBA calculations for the region of the ${}^5\text{Li}(\text{g.s.})$ resonance are shown in Fig. 2. Results are shown for laboratory scattering angles of 10° and 26° , utilizing the cluster-core potentials of Table I. Similar results were obtained at the other angles and also with the Woods-Saxon potentials given in Table I. In each case the calculated cross section was folded with an experimental energy resolution, the value of which was derived from the measured width of the nearby narrow ($\Gamma = 24$ keV) ${}^4\text{He}(\alpha,d){}^6\text{Li}$ first excited state. These energy resolution values were typically between 1.5 and 2 MeV. Due to the sufficiently small experimental angular resolution (see Sec. II), the calculated cross sections were not folded over the experimental acceptance angle. By normalizing the calculations arbitrarily to the measured ${}^5\text{Li}(\text{g.s.})$ peaks, good overall agreement is obtained. This is an indication that mechanisms not treated by the DWBA, such as knockout and multistep processes, do not contribute significantly in the $0 \leq \epsilon \leq 6$ MeV energy region. This result is in agreement with previous investigations of the ${}^4\text{He}(\alpha,{}^3\text{He}){}^5\text{He}(\text{g.s.})$ reaction [1,2].

In a study of the ${}^4\text{He}({}^7\text{Li},{}^6\text{Li}){}^5\text{He}$ and ${}^4\text{He}({}^7\text{Li},{}^6\text{He}){}^5\text{Li}$ stripping reactions at an incident energy of 50 MeV [16,17], it was shown that the ground-state resonances in ${}^5\text{Li}$ and ${}^5\text{He}$ can also be well reproduced by means of R -matrix

analysis. The optimal R -matrix fits to the measured data yield a spectroscopic factor of 0.97 for the $1p_{3/2}$ state in the mass-5 nuclei, referring here to a previous theoretical study also done by the same authors [18]. This value is in reasonably good agreement with the value of 0.925 (see Sec. V) of the present study. No angular distribution measurements nor DWBA analyses, however, were done for these reactions.

The angular distributions of the energy-integrated differential cross sections for the ${}^4\text{He}(\alpha,t){}^5\text{Li}(\text{g.s.})$ reaction at incident energies of 120, 160, and 200 MeV are shown in Figs. 3, 4, and 5, respectively. DWBA calculations employing cluster-core potentials as well as calculations employing 6-parameter Woods-Saxon potentials yield reasonable qualitative predictions of the measured data. The calculated zero-range cross sections were normalized to the measured data (employing χ -square minimization) in order to extract experimental D_0^2 factors. These values are compared with theoretical D_0^2 values in Table II. The agreement is generally satisfactory for both types of optical potentials, with the average of the theoretical values only $\sim 20\%$ higher than the average of the experimental values in each case. There may therefore still be an indication of overprediction by the DWBA but clearly less than in the earlier studies [1,2].

Sensitivity to the optical potential parameters that de-

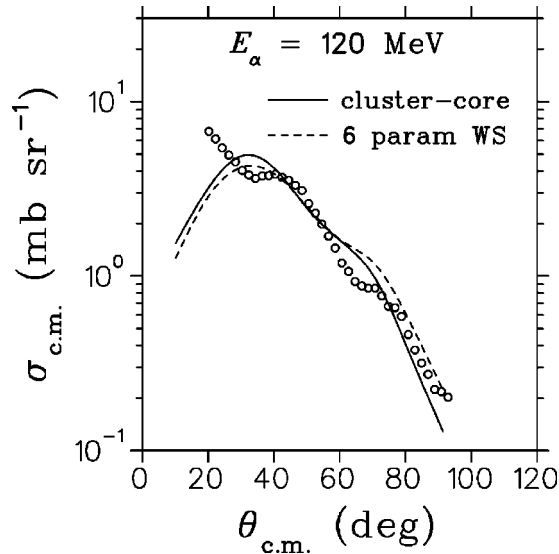


FIG. 3. Center of mass differential cross sections for the ${}^4\text{He}(\alpha,t){}^5\text{Li}(\text{g.s.})$ reaction at an incident energy of 120 MeV. Both measured and calculated DWBA cross sections for this reaction have been integrated over the triton energy region corresponding to $0 \leq \epsilon \leq 6$ MeV for central rays. The parameters for the optical potential sets CC120 and WS120 are as presented in Table I. Calculated cross sections have been normalized to the measured data and extracted D_0^2 values are presented in Table II. Statistical error bars are less than the symbol size.

scribe the α -nucleon unbound system was investigated by changing the value of the radius parameter r_1 (see Table I) arbitrarily, followed by readjustment of the well depth V_1 to correctly relocate the resonance energy of the ground state (see Sec. V). It was found that this only introduced marginal variations in the calculated cross sections, e.g., a 10% reduction of the radius parameter (leading to a value of 53 MeV for V_1) yields calculated cross sections within 6% of those found with the parameter set of Table I. Thus, to a large

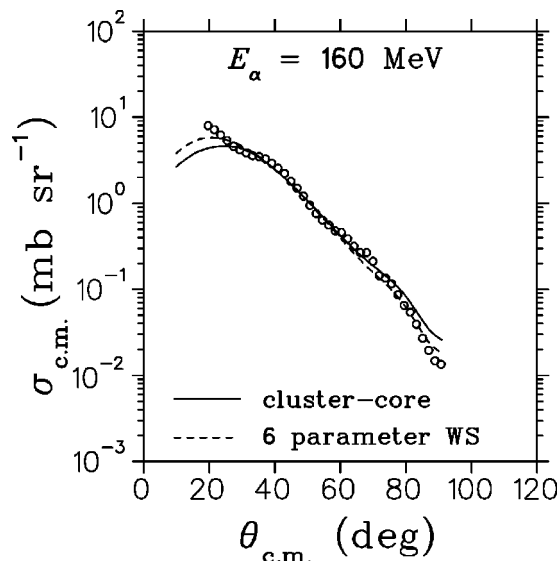


FIG. 4. Center of mass differential cross sections for the ${}^4\text{He}(\alpha,t){}^5\text{Li}(\text{g.s.})$ reaction at an incident energy of 160 MeV. The parameters for the optical potential sets CC160 and WS160 are as presented in Table I. See Fig. 3 caption for further details.

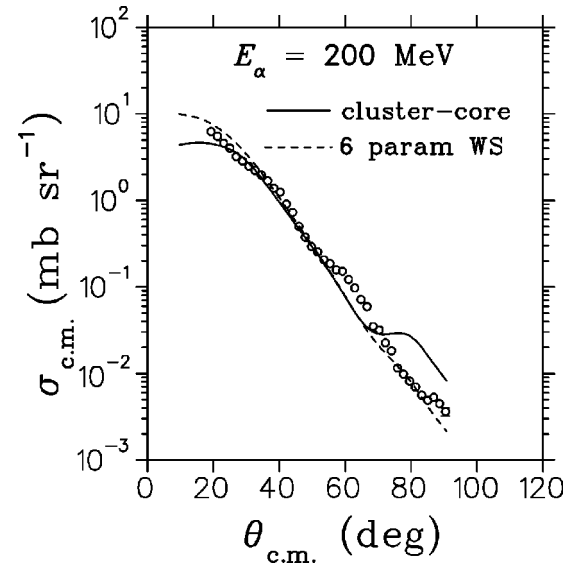


FIG. 5. Center of mass differential cross sections for the ${}^4\text{He}(\alpha,t){}^5\text{Li}(\text{g.s.})$ reaction at an incident energy of 200 MeV. The parameters for the optical potential sets CC200 and WS200 are as presented in Table I. See Fig. 3 caption for further details.

extent the calculations are found to be insensitive with regard to the details of the α -nucleon system as treated in the present DWBA calculations.

This study shows that the angular distributions of the ${}^4\text{He}(\alpha,t){}^5\text{Li}(\text{g.s.})$ reaction at incident energies between 120 and 200 MeV are very similar to corresponding results of previous studies on the ${}^4\text{He}(\alpha,{}^3\text{He}){}^5\text{He}(\text{g.s.})$ reaction. A simple rescaling of the experimental D_0^2 factors previously obtained in the ${}^4\text{He}(\alpha,{}^3\text{He}){}^5\text{He}(\text{g.s.})$ reaction study [2], based on the calculated spectroscopic factors of the present work, improves (but not entirely eliminates) the earlier discrepancy also for that reaction. In order to provide a direct comparison of the two reactions, the corresponding D_0^2 values for the ${}^4\text{He}(\alpha,{}^3\text{He}){}^5\text{He}(\text{g.s.})$ reaction obtained by using the optical parameters of Table I and the experimental results of Refs. [1,2] are also shown in Table II. On average, the agreement between experimental and theoretical results is found to be somewhat better for the ${}^4\text{He}(\alpha,t){}^5\text{Li}(\text{g.s.})$ reaction.

VII. SUMMARY AND CONCLUSIONS

Parameters for cluster-core potentials have been extracted that yield better overall agreement between theory and experimental data, both for elastic scattering as well as for the single-nucleon transfer reactions when two α particles interact. By including spectroscopic factors calculated from wave functions obtained in a large multi- $\hbar\omega$ shell model space in the DWBA calculations, the problem of overprediction of the absolute cross section values encountered in previous studies of the ${}^4\text{He}(\alpha,{}^3\text{He}){}^5\text{He}(\text{g.s.})$ reaction is improved. As a result, good agreement has been found between experimental and theoretical D_0^2 values for the ${}^4\text{He}(\alpha,t){}^5\text{Li}(\text{g.s.})$ reaction, while better agreement is also evident for the ${}^4\text{He}(\alpha,{}^3\text{He}){}^5\text{He}(\text{g.s.})$ reaction if the more realistic spectroscopic factors are taken into account.

The similarity between the absolute magnitudes of the cross sections predicted by the two very different sets of

TABLE II. Experimental and theoretical D_0^2 values for the ${}^4\text{He}(\alpha, t){}^5\text{Li}(\text{g.s.})$ and the ${}^4\text{He}(\alpha, {}^3\text{He}){}^5\text{He}(\text{g.s.})$ reactions.

E_α (MeV)	Pot. set	$D_0^2/10^4$ (MeV ² fm ³)			
		${}^4\text{He}(\alpha, t){}^5\text{Li}(\text{g.s.})$		${}^4\text{He}(\alpha, {}^3\text{He}){}^5\text{He}(\text{g.s.})$	
		Theoretical	Experimental	Theoretical	Experimental
120	CC120	3.37	3.0	3.41	2.7
	WS120	2.81	2.0	2.55	1.2
160	CC160	3.90	2.8	4.55	2.1
	WS160	3.49	2.7	4.44	2.1
200	CC200	4.50	4.1	4.59	3.7
	WS200	3.82	3.8	5.0	3.6

optical potentials is a clear indication of a surprisingly small sensitivity to the specific choice of parametrization. This, in turn, suggests that using potentials in the exit channel that are extracted for the entrance channel is a reasonable procedure in this case.

The reasonable agreement between experimental and theoretical results found in this work suggests that the discrepancy noted earlier for a similar reaction may not be signifi-

cant beyond a need to refine the inherent accuracy of the usual DWBA treatment employed in these studies.

ACKNOWLEDGMENTS

The authors wish to thank Prof. S. M. Perez for a fruitful discussion on cluster-core optical potentials.

-
- [1] R. E. Warner, J. M. Fetter, R. A. Swartz, A. Okihana, T. Konishi, T. Yoshimura, P. D. Kunz, M. Fujiwara, K. Fukunaga, S. Kakigi, T. Hayashi, J. Kasagi, and N. Koori, *Phys. Rev. C* **49**, 1534 (1994).
 - [2] G. F. Steyn, S. V. Förtsch, J. J. Lawrie, F. D. Smit, R. T. Newman, A. A. Cowley, and R. Lindsay, *Phys. Rev. C* **54**, 2485 (1996).
 - [3] F. Ajzenberg-Selove, *Nucl. Phys.* **A490**, 1 (1988).
 - [4] B. Buck, A. C. Merchant, and S. M. Perez, *Nucl. Phys.* **A614**, 129 (1997).
 - [5] P. Schwandt, SNOOPY8—Optical Potential Code for Elastic Scattering Analysis, Indiana University Cyclotron Facility Report No. 82-3 (1982).
 - [6] P. Darriulat, G. Igo, H. G. Pugh, and H. D. Holmgren, *Phys. Rev.* **137**, 315 (1965).
 - [7] P. E. Frisbee, Ph.D. thesis, University of Maryland, 1972.
 - [8] F. Michel, J. Albinski, P. Belery, Th. Delbar, Gh. Grégoire, B. Tasiaux, and G. Reidemeister, *Phys. Rev. C* **28**, 1904 (1983).
 - [9] P. Schwandt, H. O. Meyer, W. W. Jacobs, A. D. Bacher, S. D. Vigdor, and T. R. Donoghue, *Phys. Rev. C* **26**, 55 (1982).
 - [10] P. D. Kunz and E. Rost, in *Computational Nuclear Physics 2 — Nuclear Reactions*, edited by K. Langanke, J. A. Maruhn, and S. E. Koonin (Springer-Verlag, New York, 1993), p. 88.
 - [11] P. D. Kunz, A. Saha, and H. T. Fortune, *Phys. Rev. Lett.* **43**, 341 (1979).
 - [12] C. M. Vincent and H. T. Fortune, *Phys. Rev. C* **2**, 782 (1970).
 - [13] P. D. Kunz, computer code DWUCK5 (unpublished).
 - [14] D. C. Zheng, B. R. Barrett, J. P. Vary, W. C. Haxton, and C.-L. Song, *Phys. Rev. C* **52**, 2488 (1995).
 - [15] D. R. Tilley, H. R. Weller, and G. M. Hale, *Nucl. Phys.* **A541**, 1 (1992).
 - [16] C. L. Woods, F. C. Barker, W. N. Catford, L. K. Fifield, and N. A. Orr, *Aust. J. Phys.* **41**, 525 (1988).
 - [17] F. C. Barker, *Aust. J. Phys.* **41**, 743 (1988).
 - [18] F. C. Barker and C. L. Woods, *Aust. J. Phys.* **38**, 563 (1985).